Environmental Science & Technology

pubs.acs.org/est

Article

Reductive Electrochemical Activation of Hydrogen Peroxide as an Advanced Oxidation Process for Treatment of Reverse Osmosis Permeate during Potable Reuse

Cindy Weng,[§] Yi-Hsueh Chuang,[§] Bradley Davey, and William A. Mitch*

Cite This: *Environ. Sci. Technol.* 2020, 54, 12593−12601

Read Online

ACCESS | Metrics &More | Article Recommendations | Supporting Information

ABSTRACT: The UV/hydrogen peroxide (H_2O_2) advanced oxidation process (AOP) frequently employed to generate hydroxyl radical ($^{\bullet}OH$) to treat reverse osmosis permeate (ROP) in potable reuse treatment trains is inefficient, using only 10% of the H_2O_2. This study evaluated $^{\bullet}OH$ generation by electron transfer from a low-cost stainless steel cathode. In deionized water, the electrochemical system achieved 0.5 log removal of 1,4-dioxane, a benchmark for AOP validation for potable reuse, within 4 min using only 1.25 mg/L H_2O_2. Hydrogen peroxide and 1,4-dioxane degradations were maximized near −0.18 and + 0.02 V versus standard hydrogen electrode, respectively. Degradations of positively and negatively charged compounds were comparable to neutral 1,4-dioxane, indicating that degradation occurs by $^{\bullet}OH$ generation from neutral H_2O_2 and that electrostatic repulsion of contaminants from the electrode is not problematic. For ROP without chloramines, 0.5 log 1,4-dioxane removal was achieved in 6.7 min with 7 mM salts for ionic strength and 2.5 mg/L H_2O_2. For ROP with 1.4 mg/L as Cl_2 chloramines, 0.5 log 1,4-dioxane removal was achieved in 13.2 min with 7 mM salts and 4.5 mg/L total H_2O_2 dosed in three separate injections in 5 min intervals. Initial estimates based on lab-scale electrochemical AOP treatment indicated that, except for the cost of salts, the electrochemical AOP featured lower reagent costs than the UV/H_2O_2 AOP but higher electricity costs that could be reduced by optimization of the electrochemical design.

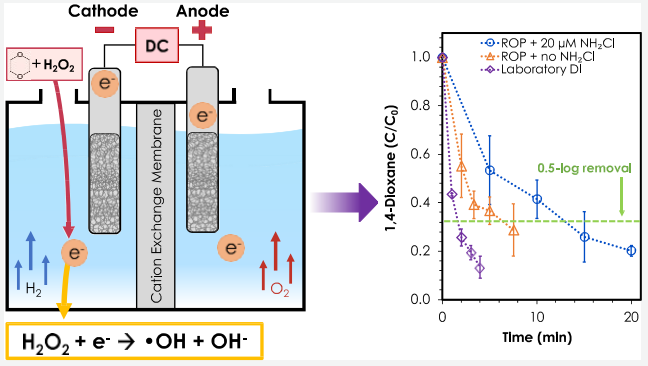

INTRODUCTION

Advanced treatment trains for the potable reuse of municipal wastewater frequently combine reverse osmosis (RO) and advanced oxidation processes (AOPs) as dual barriers against pathogens and chemical contaminants.[1,2] RO serves as a broad-screen physical barrier, typically removing >90% of chemical contaminants, particularly charged compounds over 100 Da.[2,3] AOPs serve as a broad-screen chemical barrier by generating hydroxyl radical ($^{\bullet}OH$), which reacts with a wide array of chemicals with rate constants near the diffusion limit.[4] The UV/hydrogen peroxide (UV/H_2O_2) AOP is the most commonly employed AOP in reuse trains;[1,2] this AOP generates $^{\bullet}OH$ by H_2O_2 photolysis using 254 nm light (eq 1). The ability to achieve 0.5 log removal of 1,4-dioxane, a constituent of certain chlorinated solvents and personal care products, has served as one criterion for validating AOP performance.[2,5]

$$H_2O_2 + h\nu \rightarrow 2^{\bullet}OH \quad (1)$$

The UV/H_2O_2 AOP exhibits several drawbacks. First, $^{\bullet}OH$ production from UV photolysis of H_2O_2 is inefficient because H_2O_2 features a low molar absorption coefficient at 254 nm (ε_{254} = 18.6 M^{-1} cm^{-1}).[6] The limited absorbance necessitates a high UV fluence (≥700 mJ/cm^2) to achieve the 0.5 log 1,4-dioxane removal target.[1,2,7,8] Even with such high fluence, only ∼10% of the 3−5 mg/L H_2O_2 applied is consumed,[8,9] indicating that much of the cost of H_2O_2 supply is wasted. Second, given the inefficient UV absorption by H_2O_2, applications are typically limited to high UV transmittance waters (i.e., RO permeate) to avoid competition for photon absorption. Regardless, the chloramines applied to mitigate biofouling on RO membranes act as potent scavengers of UV photons (e.g., ε_{254} = 371 M^{-1} cm^{-1} for monochloramine (NH_2Cl)).[8] Third, when chlorine is added to final effluents to leave chlorine or chloramine residuals for distribution, the residual ∼90% H_2O_2 exerts a significant chlorine demand (eq 2), thereby raising the cost of chlorine addition.[8]

$$H_2O_2 + HOCl \rightarrow O_2 + H_2O + H^+ + Cl^- \quad (2)$$

Received: April 6, 2020
Revised: August 20, 2020
Accepted: August 21, 2020
Published: August 21, 2020

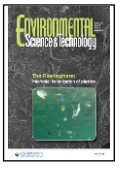

Although electrochemical AOPs represent a UV-free alternative route to radical production, most research has focused on anodic, oxidative electrochemical processes. In these processes, •OH can be generated by water oxidation when anodic potentials are ~2 V versus standard hydrogen electrode (S.H.E.) (eq 3).[10,11] Direct contaminant oxidation by electron transfer at the anode can supplement oxidation by •OH. However, anodic AOPs use expensive materials (e.g., boron-doped diamond and doped TiO_2) that feature low stability (i.e., delamination from support materials).[10,12] Contaminant treatment frequently requires hours,[10] which is longer than needed to treat continuous wastewater flows. At ~2 V versus S.H.E., chloride oxidation could produce undesirable chlorinated byproducts (e.g., chlorate and chlorinated organic byproducts).[10] These factors have hindered anodic AOP applications in full-scale treatment systems.

$$H_2O \rightarrow {}^{\bullet}OH + H^+ + e^- \quad (3)$$

Fenton processes generate •OH via H_2O_2 reduction by ferrous iron (eq 4) but require low pH (~3) and feature high costs for supplying ferrous iron and disposing $Fe(OH)_3$ sludge.[10] Electro-Fenton AOPs regenerate ferrous iron by ferric iron reduction at a cathode (eq 5), which reduces the required iron concentration to catalytic levels (~0.1 mM).[13] Although electro-Fenton processes can degrade contaminants over ~5−10 min timescales, they require low pH (~2.5−3.5) for optimal iron speciation.[13] A constant supply of iron is needed for treating continuous waste streams since dissolved iron is washed into the effluent.[13,14] Despite the lower iron concentrations, electro-Fenton AOPs would still produce ~4000 kg/day of $Fe(OH)_3$ for a facility treating ~400 ML/day of wastewater. Accordingly, electro-Fenton AOPs may be more suitable for batch treatment of smaller industrial waste volumes.

$$Fe^{2+} + H_2O_2 \rightarrow Fe^{3+} + {}^{\bullet}OH + OH^- \quad (4)$$

$$Fe^{3+} + e^- \rightarrow Fe^{2+} \quad (5)$$

Previous research employed cyclic voltammetry to demonstrate H_2O_2 reduction at pH 5.8 using a 304 grade stainless steel cathode starting at about +0.05 V versus S.H.E. with a maximum at −0.15 V versus S.H.E.;[15] however, a two-electron reduction to H_2O was assumed without demonstrating the potential for •OH production (eq 6).[4] This study evaluates •OH generation by direct electron transfer from a low-cost stainless steel cathode to H_2O_2 as an alternative AOP for treating RO permeate in potable reuse treatment trains. We focused on 0.5 log (68%) 1,4-dioxane removal as a performance benchmark to enable comparison to the UV/H_2O_2 AOP, the current industry standard. The target was to achieve this benchmark within 15 min, a reasonable timescale for a process unit within a full-scale potable reuse system treating a continuous flow. In addition to assessing 1,4-dioxane and H_2O_2 removal, this study characterized the effects of operating parameters (e.g., H_2O_2 requirements) and water quality conditions relevant to RO permeate (e.g., ionic strength and residual chloramines).

$$e^- + H_2O_2 \rightarrow {}^{\bullet}OH + OH^- \quad (6)$$

MATERIALS AND METHODS

Materials. H_2O_2 (30% v/v) and sodium hypochlorite (~5%) were purchased from Fisher Scientific. Stock solutions in deionized water were standardized using a Cary 60 UV−visible spectrophotometer at 254 nm for H_2O_2 (ε_{254nm} = 18.6 M^{-1} cm^{-1})[6] and 292 nm for hypochlorite (ε_{292nm} = 365 M^{-1} cm^{-1}).[16] 1,4-Dioxane (99.8%) and cyclohexylamine (99%) were purchased from Acros Organics (Geel, Belgium). 1,4-Dioxane-d_8 (99%), dimethyl sulfoxide (DMSO; 99.9%), and cyclohexanecarboxylic acid (98%) were purchased from Sigma-Aldrich (St. Louis, MO). Sheet graphite (0.13 mm thickness, catalog number 43078) was purchased from Alfa Aesar (Ward Hill, MA).

RO permeates typically contain ~1.5 mg/L as Cl_2 (~20 μM) chloramine residual[17] associated with chloramines applied upstream to control biofouling. Since we expected chloramines to compete with H_2O_2 for consumption of electrons, we produced RO permeate by laboratory-scale treatment of secondary municipal wastewater effluent, enabling the exclusion of chloramines to isolate their impact. Grab samples of nitrified secondary effluent were collected upstream of any disinfectant addition. Samples were filtered through glass fiber filters and stored at 4 °C. Samples were treated by RO using a laboratory-scale crossflow RO system with three plate-and-frame membrane cell units operated in parallel with the RO reject recirculated to a temperature-controlled feed tank, as described previously.[18] A Hydranautics (Oceanside, CA) ESPA-DHR RO flat-sheet membrane coupon (92 mm × 145 mm) was used in each cell; Hydranautics recommends this membrane for potable reuse trains. The membranes were pretreated by soaking in deionized water and were compacted within the crossflow unit by applying deionized water at 2.4 L/min and 17.2 bar for 6 h. The filtered wastewater was then employed as the RO feed under the same conditions, and the RO permeate (ROP) was collected. The ROP was supplemented with phosphate buffer with or without 20 μM chloramines, produced by adding ammonium chloride and sodium hypochlorite; the chloramine concentration was validated by the DPD colorimetric method.[19]

Electrolysis. Electrolysis was conducted using a dual-cell laboratory system. Except where noted, the system consisted of a 150 mL glass cathode and anode chambers separated by a cation-exchange membrane (Ultrex CMI-7000, Membranes International, Ringwood, NJ; Figure S1). The anode was filled with 2 mM phosphate buffer at pH 7.0, while the cathode was maintained at pH 5.8, with either 2 or 7 mM phosphate buffer concentrations; pH 5.8 was targeted since that is similar to the pH for municipal wastewater after treatment by RO in potable reuse facilities.[7−9] Measurements at the end of experiments verified that the pH changed by <0.2 units. Both chambers were stirred with Teflon-coated magnetic stir bars. Scotch-Brite 20 g stainless steel scrubbers (catalogue number 214C, 3 M Company, St. Paul, MN, USA; 80 cm^2/g specific surface area) were cut to various sizes for the cathode and 10.5 g for the anode and rinsed with deionized water. An Ag/AgCl reference electrode (CHI111, porous Teflon tip, CH Instruments, Austin, TX) was placed in the center of the cathode ~3 mm from the stainless steel threads; a porous frit on the reference electrode prevented direct contact with the cathode. A CH600D potentiostat (CH Instruments, Austin, TX) applied constant potentials to the cathode. A portion of the electrodes (≤10%) extended above the water surface to enable

https://dx.doi.org/10.1021/acs.est.0c02144
Environ. Sci. Technol. 2020, 54, 12593−12601

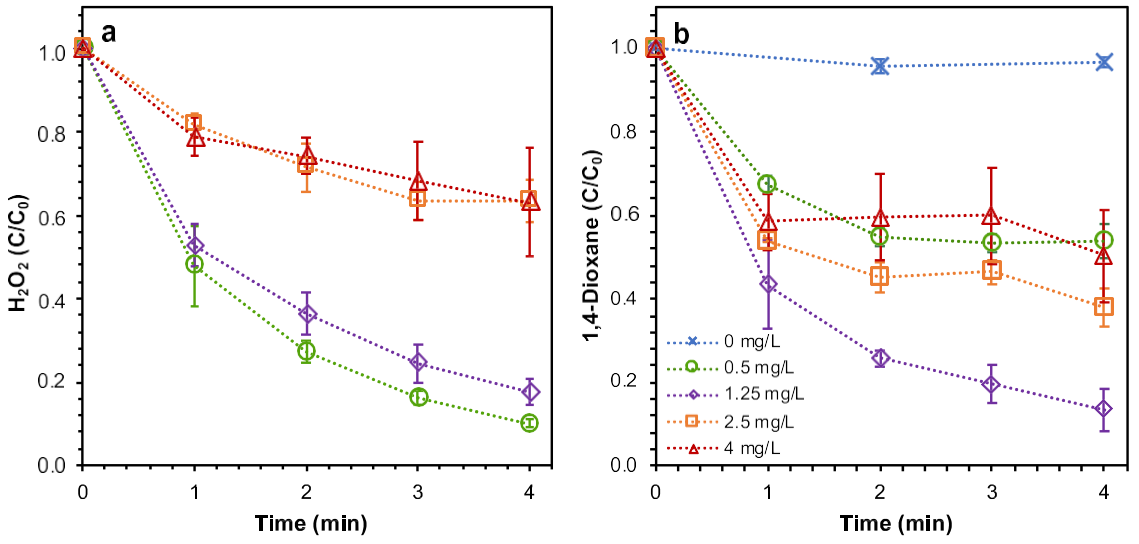

Figure 1. Degradation of (a) H_2O_2 and (b) 0.2 μM 1,4-dioxane in the cathode chamber with different initial H_2O_2 concentrations in deionized water. A constant potential of +0.02 V vs S.H.E. was applied to a 9.6 g stainless steel cathode (5.1 cm²/cm³ surface area-to-volume ratio). All experiments used 150 mL cathode and anode chambers. The cathode chamber was buffered at pH 5.8 while the anode was buffered at pH 7.0, both with 2 mM phosphate buffer. Error bars represents the range of duplicate experiments.

a connection to the potentiostat leads. The open-circuit voltage was +0.14 V. The uncompensated resistance was 5.3 Ω for 2 mM phosphate and 2.4 Ω for 7 mM phosphate. The applied potentials measured by the potentiostat were adjusted based upon these uncompensated resistances. For example, for application of +0.1 V versus an S.H.E. to the cathode in 2 mM phosphate buffer, the current was −5.5 mA such that the corrected potential applied to the cathode was +0.02 V versus S.H.E.

Prior to each experiment, the cathode required ∼100 s (or longer for certain applied voltages) to polarize and stabilize at the target potential throughout the electrode; these stable conditions are relevant to future full-scale applications, treating RO permeate continuously. Longer times were needed in the interior of the cathode, and hence we located the reference electrode in its center. Prior to spiking H_2O_2 and the organic contaminant and throughout the experiments, we validated that the cathode had achieved and remained at the target potential by measuring the potential between the cathode and reference electrode using a multimeter. After spiking, samples (7 mL) were periodically removed from the cathode for analysis for residual H_2O_2, 1,4-dioxane, or other target contaminants. Up to five samples were collected such that the total volume of sample removed (35 mL) was <25% of the cathode solution. All experiments were conducted at least in duplicate.

Analytical Methods. Residual H_2O_2 was measured by its oxidation of DPD dye catalyzed by peroxidase enzyme.[20] 1,4-Dioxane was extracted into methyl *tert*-butyl-ether (MtBE) and analyzed by gas chromatography mass spectrometry (GC/MS), as detailed previously (Text S1).[7] Formaldehyde was analyzed by the US EPA Method 556. Cyclohexanecarboxylate was analyzed by GC/MS after extraction into MtBE and methylation using acidic methanol following the US EPA method 552.3. Cyclohexylammonium was analyzed by liquid chromatography mass spectrometry. Text S1 provides additional details.

RESULTS

Effects of H_2O_2 Concentration. Initial experiments evaluated the effect of 0−4 mg/L H_2O_2 on 0.2 μM 1,4-dioxane degradation in deionized water buffered at pH 5.8 (relevant to RO permeate) when +0.02 V versus S.H.E. was applied to the 9.6 g cathode (Figure 1). This mass of stainless steel corresponds to a 770 cm² surface area or a surface area-to-volume ratio with respect to the 150 mL cathode chamber of 5.1 cm²/cm³. The 0.2 μM (18 μg/L) 1,4-dioxane concentration is comparable to the low levels expected in RO permeate and below the 0.5−4 mg/L (15−120 μM) H_2O_2 concentrations evaluated; because H_2O_2 and 1,4-dioxane compete to react with $^{\bullet}OH$, it is important to maintain a relevant concentration ratio to represent this competition.

For 0.5 mg/L H_2O_2, H_2O_2 decay was 90% (0.45 mg/L) over 4 min (Figure 1a). The percent removal of H_2O_2 declined with increasing dose, from 82% (1 mg/L degraded) for 1.25 mg/L to 37% (1.5 mg/L degraded) for 4 mg/L. Although first-order kinetics was observed for 0.5 and 1.25 mg/L H_2O_2, the <50% loss of H_2O_2 prevented the characterization of the order of degradation kinetics for 2.5 and 4 mg/L H_2O_2. However, the plateau in the absolute concentration of H_2O_2 degraded with increasing H_2O_2 dose suggests that the kinetics shift from first order for 0.5 mg/L toward zero order with increasing dose, thereby suggesting that electron transfer from the electrode to H_2O_2 becomes limiting with increasing H_2O_2 concentration. For 1,4-dioxane, degradation was <2% over 4 min without H_2O_2 (Figure 1b). For 0.5−4 mg/L H_2O_2, 1,4-dioxane degradation was 46−87% after 4 min, with maximum degradation observed for 1.25 and 2.5 mg/L H_2O_2. Only the 1.25 mg/L H_2O_2 conditions reached the 0.5 log 1,4-dioxane removal target by achieving 0.87 log removal within 4 min.

The degradation of 1.25 mg/L H_2O_2 and 0.2 μM 1,4-dioxane was evaluated using 150 mL electrode chambers and a 2.5 g stainless steel cathode (1.3 cm²/cm³) at pH 5.8, while the potential applied to the cathode varied from −0.38 to +0.32 V versus S.H.E. Over a 4 min timescale, H_2O_2 and 1,4-dioxane degradation were the highest at −0.18 and +0.02 V, with much lower degradation at −0.38 and +0.32 V (Figure 2),

https://dx.doi.org/10.1021/acs.est.0c02144
Environ. Sci. Technol. 2020, 54, 12593−12601

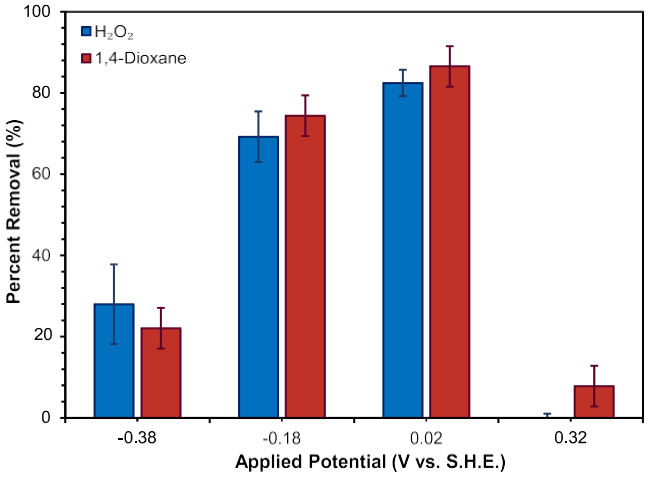

Figure 2. Degradation of 1.25 mg/L H_2O_2 and 0.2 μM 1,4-dioxane in the cathode chamber with different potentials (vs. S.H.E.) applied to a 2.5 g stainless steel cathode (1.3 cm^2/cm^3) in deionized water after 4 min. All experiments used 150 mL cathode and anode chambers. The cathode chamber was buffered at pH 5.8, while the anode was buffered at pH 7.0, both with 2 mM phosphate buffer. Error bars represent the range of duplicate experiments.

respectively. At +0.02 V, the current was 5.8 mA after H_2O_2 and 1,4-dioxane injection, resulting in a 0.03 mA/cm^2 current density for the 200 cm^2 cathode surface area. A previous cyclic voltammetry study using a stainless steel cathode indicated that H_2O_2 reduction commenced at about +0.05 V with maximum reduction occurring near −0.15 V.[15] We adjusted the standard reduction potential for proton reduction (eq 7) by water splitting to pH 5.8 via the Nernst equation (eq 8), where n is the number of electrons transferred, and a is the number of protons involved in the half reaction; the resulting pH-adjusted potential is −0.34 V. Thus, at −0.18 and + 0.02 V, H_2O_2 reduction and the associated degradation of 1,4-dioxane would be favored, while at −0.38 V its degradation would be expected to decline due to competition from proton reduction. At +0.32 V, reduction of neither H_2O_2 nor protons would be favored.

$$2\,H^+ + 2\,e^- \rightarrow H_2 \quad (7)$$

$$E = E_0 - \frac{0.059}{n}\log\left(\frac{1}{[H^+]^a}\right) \quad (8)$$

Role of •OH. The finding that 1,4-dioxane degradation over 4 min increased from <2% without H_2O_2 to 87% with 1.25 mg/L H_2O_2 (Figure 1) suggests that H_2O_2-mediated degradation is the dominant mechanism for 1,4-dioxane degradation rather than direct degradation at the electrode. Electrons from the cathode have the potential to react with H_2O_2, water, or protons. Eq 9 provides the fraction of electrons that reacts with H_2O_2 (F_{H2O2}),

$$F_{H_2O_2} = \frac{k_{H_2O_2}[H_2O_2]}{k_{H_2O}[H_2O_2] + k_{H_2O}[H_2O] + k_{H^+}[H^+]} \quad (9)$$

where k_{H2O2}, k_{H2O}, and k_{H+} are the reaction rate constants of electrons with H_2O_2 (1.2 × 10^{10} M^{-1} s^{-1}), H_2O (1.0 × 10^3 M^{-1} s^{-1}), and H^+ (2.4 × 10^{10} M^{-1} s^{-1}), respectively.[21] At pH 5.8, F_{H2O2} is 65% for 0.5 mg/L (15 μM) H_2O_2 but ≥83% for ≥1.25 mg/L (37 μM) H_2O_2. Accordingly, H_2O_2 effectively competes to react with electrons.

To confirm •OH formation during cathodic reduction of H_2O_2, we evaluated formaldehyde formation from DMSO ($(CH_3)_2SO$) as a probe compound. Previous research has demonstrated that •OH reacts with DMSO to form methyl radical ($CH_3^•$; eq 10).[22−24] Dimerization of the $CH_3OO^•$ radicals formed when $CH_3^•$ reacts with oxygen released formaldehyde. The overall stoichiometry indicates consumption of 2 •OH and 2 DMSO to produce each formaldehyde (eq 11). We treated 0.5 μM DMSO and 1.25 mg/L H_2O_2 (29 μM) by applying a +0.02 V potential to the cathode. Although DMSO degradation was not monitored, it features a higher rate constant with •OH (k = 6.5 × 10^9 M^{-1} s^{-1})[21] than that with 1,4-dioxane (k = 3 × 10^9 M^{-1} s^{-1}).[21] The 0.1 μM (~3 μg/L) background formaldehyde concentration in the deionized water increased linearly to 0.3 μM after 4 min (Figure S2), while no significant formaldehyde formation was observed without H_2O_2. The 0.2 μM formation of formaldehyde was 80% of the 0.25 μM maximum expected for complete oxidation of DMSO by •OH.

$$^•OH + (CH_3)_2SO \rightarrow CH_3SOOH + CH_3^• \quad (10)$$

$$2\,^•OH + 2\,(CH_3)_2SO + O_2 \rightarrow CH_2O + CH_3OH + 2\,CH_3SOOH \quad (11)$$

The stainless steel scrubbers were 410 type stainless steel, which is ~86% iron and ~12% chromium, with only trace amounts of nickel.[25] Because these redox-active metals could shuttle electrons between the cathode and H_2O_2, we used inductively coupled plasma mass spectrometry to measure their concentrations during application of +0.02 V to the cathode (9.6 g of scrubber in a 150 mL cathode chamber at pH 5.8 with 2 mM phosphate) in the presence of 1.25 mg/L H_2O_2 and 0.2 μM 1,4-dioxane. While the concentrations of chromium (~18 μg/L) and nickel (~0.2 μg/L) did not change significantly, the concentration of iron increased linearly (Table S1), reaching 790 μg/L (14 μM) after 5.6 min. However, electron shuttling by iron was unlikely to be important because even the final iron concentration was approximately sevenfold lower than the 100 μM concentrations employed in electro-Fenton systems.[13] In additional control experiments to evaluate the potential contribution of Fenton reactions, 0.2 μM 1,4-dioxane was not degraded when treated at pH 5.8 (2 mM phosphate) in the presence of 1.25 mg/L H_2O_2 and 14 μM or 60 μM Fe^{2+}, a concentration approximately fourfold higher than the maximum iron concentration observed in our experiments (Figure S3). Moreover, when +0.02 V versus S.H.E. was applied to the cathode at pH 5.8 with 1.25 mg/L H_2O_2, the degradation of 0.2 μM 1,4-dioxane was similar (Figure S4) using a 1.3 cm^2/cm^3 stainless steel cathode and anode (0.25-log) or a 1.3 cm^2/cm^3 sheet graphite cathode with a platinum wire anode (0.21 log). The lower specific surface area (1.3 cm^2/cm^3) for these experiments was necessary due to the lower specific surface area of the sheet graphite cathode. Interestingly, the H_2O_2 concentration increased when sheet graphite was used, indicating H_2O_2 production from two-electron O_2 reduction. However, the activity of the sheet graphite was not maintained over additional use cycles, likely due to degradation from reactions with •OH.

Effect of Cathode Size. The effect of cathode size was evaluated on the basis of its surface area relative to the volume of water treated (cm^2/cm^3). Using the 150 mL cathode

https://dx.doi.org/10.1021/acs.est.0c02144
Environ. Sci. Technol. 2020, 54, 12593−12601

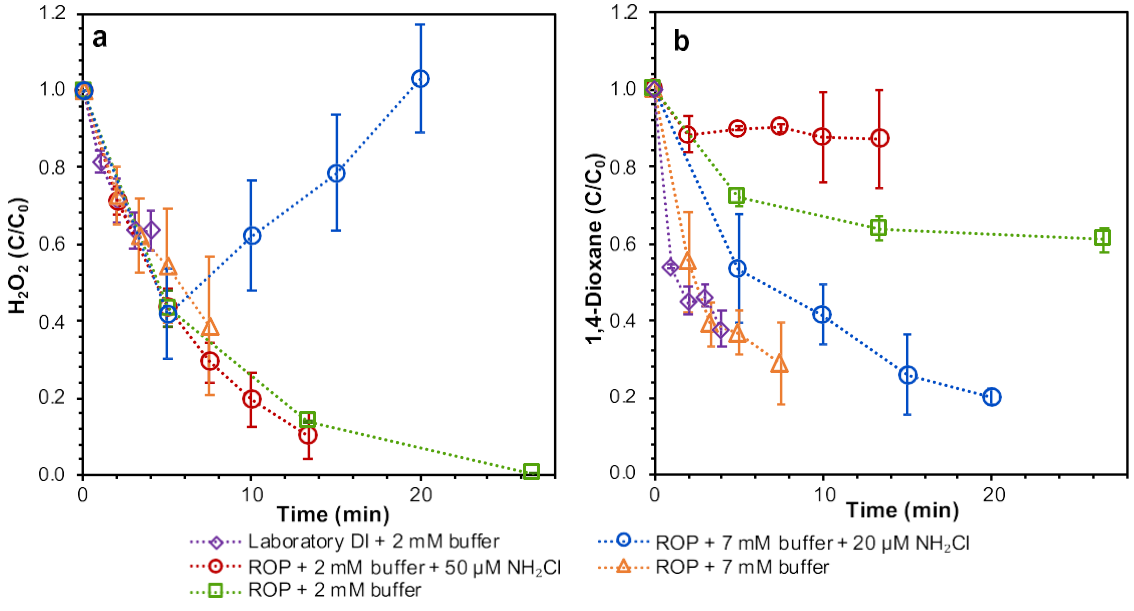

Figure 3. Degradation of (a) H_2O_2 and (b) 0.2 μM 1,4-dioxane in the cathode chamber upon application of +0.02 V vs S.H.E. to a 9.6 g stainless steel cathode (5.1 cm²/cm³) in deionized water or reverse osmosis permeate (ROP) without or with chloramines and with different concentrations of phosphate buffer at pH 5.6. The anode was buffered at pH 7.0 with 2 mM phosphate buffer. Green squares and red circles: ROP generated from sample 1. Blue circles and orange triangles: ROP generated from sample 2. Error bars represent the range of duplicate experiments.

chamber, the surface area-to-volume ratio was tested at 1.3, 2.7, 3.7, and 5.1 cm²/cm³ by using 2.5 g (200 cm²), 5 g (400 cm²), 7 g (560 cm²), and 9.6 g (770 cm²) stainless steel cathodes, respectively. The stainless steel anode was fixed at 10.5 g, corresponding to 843 cm² and a surface area-to-volume ratio with respect to the 150 mL anode chamber of 5.6 cm²/cm³. The losses of 1.25 mg/L H_2O_2 and 0.2 μM 1,4-dioxane were measured when +0.02 V was applied to the cathode at pH 5.8 (Figure S5). The percent removal of H_2O_2 and 1,4-dioxane were both ~40% for the 1.3 and 2.7 cm²/cm³ cathodes but increased to 82 and 87%, respectively, at 5.1 cm²/cm³.

Degradation of Ionic Compounds. The application of a constant potential to the cathode might affect the treatment of charged compounds by hindering or promoting their approach to the electrode by electrostatic interactions. We compared the degradation of 1,4-dioxane, which is neutral, to that of cyclohexylammonium (pK_a = 10.6) and cyclohexanecarboxylate (pK_a = 4.9) as examples of positively charged and negatively charged compounds at pH 5.8, respectively. When +0.02 V was applied to the cathode (3.9 cm²/cm³ in 200 mL chambers) with 1.25 mg/L H_2O_2 and 0.2 μM of each compound, the degradation was somewhat faster for positively charged cyclohexylammonium, reaching 76% after 3 min, compared to 60% for neutral 1,4-dioxane and 59% for negatively charged cyclohexanecarboxylate (Figure S6). Although electrostatic attraction of positively charged cyclohexylammonium to the cathode may have enhanced its degradation, the degradation of all three compounds was comparable. The formation of $^{\bullet}OH$ by electron transfer from the cathode to neutral H_2O_2 should not be affected by electrostatic interactions with the cathode. The similarity between the degradation of neutral 1,4-dioxane and negatively charged cyclohexanecarboxylate indicates that contaminants are degraded by $^{\bullet}OH$ in the bulk solution rather than direct electron transfer at the cathode.

Treatment of Reverse Osmosis Permeate. Additional experiments were conducted with RO permeate (ROP) generated by treatment of two samples of nitrified secondary municipal wastewater effluent (<0.2 mg N/L ammonia) with a laboratory-scale RO treatment system. For both sample 1 (pH 7.1, 6.7 mg/L dissolved organic carbon (DOC)) and sample 2 (pH 7.1, 7.1 mg/L DOC), RO treatment reduced the pH to 5.5 and the DOC to <0.2 mg/L. Authentic RO permeates typically contain ~1.5 mg/L as Cl_2 (~20 μM) chloramine residuals[17] from chloramines applied upstream of membrane units to control biofouling. Since chloramines were expected to compete effectively with H_2O_2 for electrons and with 1,4-dioxane for $^{\bullet}OH$, ROP production by laboratory-scale treatment of secondary effluent permitted the exclusion of chloramines to isolate their impact.

When ROP (sample 1) with 50 μM chloramines (formed by addition of 50 μM free chlorine and 60 μM ammonia) was treated with 1.25 mg/L H_2O_2 at +0.02 V with 2 mM phosphate buffer (pH 5.6), H_2O_2 degradation was comparable to that observed under the same conditions in deionized water without chloramines. However, the degradation of 0.2 μM 1,4-dioxane was much slower (compare red circles vs. purple diamonds in Figure 3), leveling out at ~12% loss after 2 min, when 71% of the H_2O_2 remained. The finding that 1,4-dioxane degradation was affected more than H_2O_2 degradation suggests that $^{\bullet}OH$ scavenging by chloramines (k_{OH} = 1.02 × 10⁹ M^{-1} s^{-1} for NH_2Cl vs. 3.1 × 10⁹ M^{-1} s^{-1} for 1,4-dioxane)[9] was more important than competition between H_2O_2 and chloramines for electrons from the cathode.

We repeated the experiment with ROP but without chloramines and with double the H_2O_2 dose (green squares in Figure 3). When ROP (sample 1) without chloramines was treated with 2.5 mg/L H_2O_2 at +0.02 V with 2 mM phosphate buffer (pH 5.6), H_2O_2 degradation was again comparable to that observed in deionized water. However, 1,4-dioxane degradation leveled out at ~35% loss after 13 min, faster than with chloramines (red circles) but slower than the deionized water experiments (purple diamonds). After 13 min, only 14% of the H_2O_2 (0.35 mg/L) remained, suggesting that

https://dx.doi.org/10.1021/acs.est.0c02144
Environ. Sci. Technol. 2020, 54, 12593−12601

the 1,4-dioxane degradation became limited by the remaining H_2O_2 concentration.

In experiments with ROP (sample 1) containing 50 μM chloramines and 2 mM phosphate buffer, we evaluated re-spiking the cathode with 1.25 mg/L H_2O_2 every 5 min for a total of 5 mg/L H_2O_2 after 20 min (red circles in Figure S7). 1,4-Dioxane degradation leveled out at ∼35% after 15 min, while the H_2O_2 concentration increased up to ∼2 mg/L after 20 min due to the repeated H_2O_2 injections. We suspected that the leveling out of 1,4-dioxane degradation might result from reduced ionic strength near the cathode surface caused by electrostatic repulsion between the cathode and buffer components. For example, we had observed that the central portion of the cathode required longer times to reach the applied potential than the cathode edges during initial charging, suggesting that the non-uniform cathode potential was associated with a non-uniform ion distribution in the adjacent medium. Thus, we repeated the experiment, but after 5 min, we turned off the potential for 20 s to relax the repulsion between the cathode and buffer components. Next, we injected an additional 1.25 mg/L H_2O_2 and then turned the potential back on for 5 min. We repeated these steps for three additional cycles (blue squares in Figure S7). While the H_2O_2 concentration profile was unchanged (i.e., increased to 2 mg/L after 20 min), 1,4-dioxane degradation reached 50% after 20 min.

Suspecting that the 1,4-dioxane degradation was limited by ionic strength, we evaluated the use of 7 mM phosphate buffer. Utilities may consider addition of salts to stabilize ROP to minimize corrosion of pipelines and leaching of arsenic and other undesirable aquifer components during ROP infiltration into groundwater for indirect potable reuse.[26,27] We considered 7 mM to be a reasonable upper limit to the ionic strength that could be added to ROP; for example, 7 mM NaCl would represent the addition of 406 mg/L total dissolved solids (TDS), lower than the 500 mg/L secondary maximum contaminant level for TDS.[28] First, we applied +0.02 V to the cathode in ROP (sample 2) buffered with 7 mM phosphate buffer without chloramines; the degradation of 2.5 mg/L H_2O_2 and 0.2 μM 1,4-dioxane were similar to that observed in deionized water buffered with 2 mM phosphate without chloramines, with 0.5 log (68%) removal of 1,4-dioxane achieved within ∼6.7 min (interpolation of orange triangles in Figure 3).

For ROP containing 20 μM chloramines (formed by addition of 20 μM free chlorine and 24 μM ammonia), we applied +0.02 V to the cathode containing 7 mM phosphate buffer with 2.5 mg/L H_2O_2 and 0.2 μM 1,4-dioxane. However, after 5 min, we turned off the potential for 20 s, injected an additional 1 mg/L H_2O_2, and then turned the potential back on for 5 min. We repeated these steps for two additional cycles. The 1 mg/L H_2O_2 re-spiking dose maintained sufficient H_2O_2 in solution without overaccumulation of H_2O_2, reaching the initial 2.5 mg/L concentration after 20 min (blue circles in Figure 3). This procedure enhanced 1,4-dioxane degradation, although degradation remained slower than without chloramines. However, interpolation between the measurements taken at 10 and 15 min indicated that 0.5 log removal of 1,4-dioxane was achieved within 13.2 min, after a total addition of 4.5 mg/L H_2O_2.

DISCUSSION

Generation of $^{\bullet}OH$ by cathodic reduction of H_2O_2 achieved 0.5 log removal of 1,4-dioxane in RO permeate within ∼7 min without chloramines and within ∼13 min with 20 μM chloramines. Both of these timescales are within the 15 min range that is feasible for treating a continuous flow of potable reuse water. Electrochemical generation of $^{\bullet}OH$ was demonstrated using DMSO as a probe. However, the fraction of the $^{\bullet}OH$ that reacts with 1,4-dioxane (F_{14D}) rather than with H_2O_2 or chloramines should be given by eq 12, where k_{14D} is the $^{\bullet}OH$ rate constant with 1,4-dioxane (3.1×10^9 M^{-1} s^{-1}),[29] k_{H2O2} is the $^{\bullet}OH$ rate constant with H_2O_2 (2.7×10^7 M^{-1} s^{-1}),[21] and k_{NH2Cl} is the $^{\bullet}OH$ rate constant with monochloramine (NH_2Cl) ($k_{NH2Cl} = 1.02 \times 10^9$ M^{-1} s^{-1}).[9] For 0.2 μM 1,4-dioxane, $F_{1,4D}$ is 24% for 2.5 mg/L H_2O_2 without chloramines and 2.7% for 2.5 mg/L H_2O_2 with 20 μM chloramines.

However, the molar degradation of 1,4-dioxane relative to the molar change in H_2O_2 (Δ[1,4-dioxane]/Δ[H_2O_2]) was only ∼0.3% without chloramines and 0.2% with 20 μM chloramines. Reduction of H_2O_2 can proceed by either one or two electron transfer pathways (eqs 6 and 13). These results suggest that only a small fraction of the H_2O_2 loss proceeds via the one-electron transfer pathway to produce $^{\bullet}OH$, and only a fraction of the $^{\bullet}OH$ produced degrades 1,4-dioxane. Although this suggests that there is significant room to improve process efficiency by favoring the one-electron transfer pathway, ∼0.5 log reduction of 1,4-dioxane was still achieved within 15 min while leaving only 1 mg/L H_2O_2 without chloramines and 2.0 mg/L H_2O_2 with chloramines. Current UV/H_2O_2 AOP systems typically apply ∼3 mg/L H_2O_2 to achieve this level of 1,4-dioxane removal while leaving at least 2.7 mg/L H_2O_2; under these circumstances Δ[1,4-dioxane]/Δ[H_2O_2] would be only ∼2%. This percentage is higher than that observed for the electrochemical system, mostly because less of the H_2O_2 is degraded in the UV/H_2O_2 AOP due to the lack of a H_2O_2 degradation pathway other than H_2O_2 photolysis; however, the greater H_2O_2 residual after UV/H_2O_2 AOP treatment also necessitates a greater chlorine dose to quench.

$$F_{1,4D} = \frac{k_{1,4D}[1,4D]}{k_{1,4D}[1,4D] + k_{H_2O_2}[H_2O_2] + k_{NH_2Cl}[NH_2Cl]} \quad (12)$$

$$H_2O_2 + 2\,e^- + 2\,H^+ \rightarrow 2\,H_2O \quad E = 1.42\ V \text{ at pH } 5.8 \quad (13)$$

We conducted an initial cost comparison between the UV/H_2O_2 and electrochemical AOPs targeting 0.5 log 1,4-dioxane removal of RO permeate. Based on previous research studies,[7,8] we assumed that a 1000 mJ/cm² UV fluence would be needed to achieve 0.5 log removal of 1,4-dioxane in the presence of 20 μM chloramines (1.4 mg/L as Cl_2) using 3.4 mg/L H_2O_2, leaving a 2.7 mg/L H_2O_2 residual. We also considered the addition of sodium bisulfite to quench residual chloramines prior to UV/H_2O_2 treatment, in which case only 360 mJ/cm² UV fluence would be needed to achieve 0.5 log removal.[8] For the electrochemical AOP, we used the experimental results for ROP treatment without and with 20 μM chloramines (orange triangles and blue circles in Figure 3). These cost estimates considered the costs to treat 1 ML of ROP, including the costs to (1) quench chloramine residuals with sodium bisulfite (if applicable), (2) add H_2O_2, (3) supply

https://dx.doi.org/10.1021/acs.est.0c02144
Environ. Sci. Technol. 2020, 54, 12593−12601

electricity, (4) add chlorine to quench residual H_2O_2, and (5) add chlorine and ammonium sulfate to provide a 35 μM (2.5 mg/L as Cl_2) chloramine residual (Table 1). Additionally, we considered the cost to supply 7 mM salt, the concentration employed for RO permeate experiments. Text S2 provides details for these estimates.

Table 1. Cost Comparison between UV/H_2O_2 and Electrochemical AOPs ($/ML)

	UV/H_2O_2 AOP		electrochemical AOP	
cost type	with NH_2Cl	NH_2Cl quenched	with NH_2Cl	NH_2Cl quenched
quenching chloramines	$	$ 2.16	$	$ 2.16
H_2O_2 addition	$ 4.95	$ 4.95	$ 6.55	$ 3.64
electricity	$ 6.35	$ 2.29	$ 12.44	$ 7.91
NaOCl for quenching H_2O_2	$ 9.73	$ 9.73	$ 6.29	$ 3.50
NaOCl to provide a residual	$ 2.92	$ 3.78	$ 3.78	$ 3.78
$(NH_4)_2S_2O_4$ to provide a residual	$ 7.64	$ 9.90	$ 9.90	$ 9.90
sub-total	$ 31.58	$ 32.80	$ 38.96	$ 30.88
salt addition	$	$	$ 35.89	$ 35.89
total	$ 31.58	$ 32.80	$ 66.77	$ 74.85

The results indicate that the cost of UV/H_2O_2 AOP treatments would be comparable without and with pretreatment with sodium bisulfite to quench chloramines. Without considering the cost of salt addition, the overall cost of electrochemical AOP treatment with initial quenching of chloramines could be comparable to UV/H_2O_2 AOP treatment. However, without chloramine quenching the overall cost would be ~20% higher. The electrochemical AOP would feature significant savings on the cost of chlorine addition to quench residual H_2O_2 since the H_2O_2 residual would be lower for the electrochemical AOP. The cost of electricity was higher for electrochemical treatment, particularly without pretreatment to quench chloramines.

However, the cost to provide 7 mM salts doubles the cost for electrochemical AOP treatment. Potable reuse facilities are considering salt addition to UV/H_2O_2 AOP effluent to reduce corrosion in distribution pipelines and the potential dissolution of toxic elements (e.g., arsenic) in natural deposits when potable reuse water is used for aquifer recharge.[26] However, this salt addition would be lower than the 7 mM considered for electrochemical AOP treatment of RO permeate. This initial analysis highlights the importance of identifying alternative methods of providing ionic strength. A potential solution that needs further evaluation is using nanofiltration (NF) instead of RO. NF would permit passage of monovalent ions, significantly reducing the salt requirement. Although the rejection of organic contaminants by the membranes might decrease, future research would need to evaluate whether the potential reduction in energy required for NF versus RO may offset the increase in energy required by the electrochemical AOP to degrade the higher organic contaminant concentrations.

This study demonstrated initial proof of concept that treatment of organic contaminants in RO permeate could be achieved via direct electron transfer from an inexpensive stainless steel cathode to H_2O_2. The electrochemical AOP achieved 0.5 log 1,4-dioxane removal in <15 min at pH relevant to RO permeate (~5.5) and at salt concentrations relevant to drinking water. If the cost of salt can be overcome (e.g., by switching to NF), then the cost of electrochemical AOP treatment would be comparable to UV/H_2O_2 AOP treatment. This is encouraging, particularly considering that the electrochemical system has not been fully optimized, while the UV/H_2O_2 system has been optimized, having been employed at full scale for at least 20 years.

Several aspects of the electrochemical system could be optimized. For example, the high electricity cost reflects a lab-scale, two-cell electrochemical system with cylindrical electrodes, wherein the distance between electrodes (~3.5 cm) has not been optimized. The cell resistance (R in Ω) scales according to eq 14, where ρ (Ω cm) is the ionic resistivity of the electrolytes, l (cm) is the spacing between the electrodes, and A (cm²) is their surface area.[30] Moreover, the long time required to reach the target potential within the interior of the cathode scrubber likely reflects polarization of the electrolyte within its cylindrical interiors (e.g., by electrostatic repulsion of anions), which would be less important in flatter electrodes. We used these porous, cylindrical scrubbers because they provided a higher surface area than flat stainless steel plates. A full-scale system would likely use parallel plates, where the full-cell voltage and associated energy cost should be much less due to the closer spacing of the electrodes and their flatter shapes. However, the design of porous stainless steel electrodes and their configuration needs optimization.

$$R = \rho \frac{l}{A} \tag{14}$$

Similarly, this study employed commercially available kitchen scrubbers (Scotch-Brite stainless steel scrubbers) constructed from 410 type stainless steel because of their low cost. Even though the concentrations of iron shed from the stainless steel electrodes were at least sevenfold lower than those employed for electro-Fenton treatment,[13] the shedding rate would deplete ~10% of the iron in four weeks of continuous treatment. Although carbon materials could avoid release of metals, we observed rapid degradation of a sheet graphite cathode, likely from hydroxyl radical reactions with the graphite. A platinum anode would avoid oxidative degradation, but identifying lower-cost materials is important to render the process economically feasible. Future research can evaluate whether alternative stainless steel types or other lower-cost materials could exhibit lower degradation and enhance the process efficiency by favoring one-electron reduction of H_2O_2 over the two-electron pathway.

If the costs and efficiency of electrochemical AOP treatment can be further improved, then this electrochemical treatment could be attractive relative to the UV/H_2O_2 AOP. For example, an electrochemical AOP could treat waters with lower UV transmittance (UVT). These waters include conventional drinking waters and the RO-free potable reuse trains (e.g., trains based on ozone/biological activated carbon),[31] gaining favor in inland regions due to the difficulty associated with RO concentrate disposal. Both waters feature higher salinity than RO permeate, thereby reducing the cost associated with salt addition to boost ionic strength.

https://dx.doi.org/10.1021/acs.est.0c02144
Environ. Sci. Technol. 2020, 54, 12593−12601

ASSOCIATED CONTENT

Supporting Information

The Supporting Information is available free of charge at https://pubs.acs.org/doi/10.1021/acs.est.0c02144.

Analytical details, reactor schematic, formaldehyde formation, control experiments on the potential importance of Fenton reactions, effect of turning the potential on and off, full-cell voltage and current during ROP treatment, metal concentrations, and cost estimate details (PDF)

AUTHOR INFORMATION

Corresponding Author

William A. Mitch − *Department of Civil and Environmental Engineering, Stanford University, Stanford, California 94305, United States;* orcid.org/0000-0002-4917-0938; Phone: 650-725-9298; Email: wamitch@stanford.edu; Fax: 650-723-3505

Authors

Cindy Weng − *Department of Civil and Environmental Engineering, Stanford University, Stanford, California 94305, United States*

Yi-Hsueh Chuang − *Department of Civil and Environmental Engineering, Stanford University, Stanford, California 94305, United States; Institute of Environmental Engineering, National Chiao Tung University, Hsinchu City 30010, Taiwan;* orcid.org/0000-0002-9128-8200

Bradley Davey − *Department of Civil and Environmental Engineering, Stanford University, Stanford, California 94305, United States*

Complete contact information is available at: https://pubs.acs.org/10.1021/acs.est.0c02144

Author Contributions

§C.W. and Y.-H.C. contributed equally to this work.

Notes

The authors declare the following competing financial interest(s): We have filed for patent protection.

ACKNOWLEDGMENTS

C.W. was supported by the Gates Millennium Fellowship.

REFERENCES

(1) Gerrity, D.; Pecson, B.; Trussell, R. S.; Trussell, R. R. Potable Reuse Treatment Trains throughout the World. *J. Water Supply Res. Technol. - AQUA* 2013, *62*, 321−338.

(2) Marron, E. L.; Mitch, W. A.; von Gunten, U.; Sedlak, D. L. A Tale of Two Treatments: The Multiple Barrier Approach to Removing Chemical Contaminants during Potable Water Reuse. *Acc. Chem. Res.* 2019, *52*, 615−622.

(3) Agus, E.; Sedlak, D. L. Formation and Fate of Chlorination By-Products in Reverse Osmosis Desalination Systems. *Water Res.* 2010, *44*, 1616−1626.

(4) Buxton, G. V.; Greenstock, C. L.; Helman, W. P.; Ross, A. B. Critical Review of Rate Constants for Reactions of Hydrated Electrons, Hydrogen Atoms and Hydroxyl Radicals (·OH/·O⁻) in Aqueous Solution. *J. Phys. Chem. Ref. Data* 1988, *17*, 513−886.

(5) Godri Pollitt, K. J.; Kim, J.-H.; Peccia, J.; Elimelech, M.; Zhang, Y.; Charkoftaki, G.; Hodges, B.; Zucker, I.; Huang, H.; Deziel, N. C.; Murphy, K.; Ishii, M.; Johnson, C. H.; Boissevain, A.; O'Keefe, E.; Anastas, P. T.; Orlicky, D.; Thompson, D. C.; Vasiliou, V. 1,4-Dioxane as an Emerging Water Contaminant: State of the Science and Evaluation of Research Needs. *Sci. Tot. Environ.* 2019, *690*, 853−866.

(6) Morgan, M. S.; Van Trieste, P. F.; Garlick, S. M.; Mahon, M. J.; Smith, A. L. Ultraviolet Molar Absorptivities of Aqueous Hydrogen Peroxide and Hydroperoxyl Ion. *Anal. Chim. Acta* 1988, *215*, 325−329.

(7) Zhang, Z.; Chuang, Y. H.; Szczuka, A.; Ishida, K. P.; Roback, S.; Plumlee, M. H.; Mitch, W. A. Pilot-Scale Evaluation of Oxidant Speciation, 1,4-Dioxane Degradation and Disinfection Byproduct Formation during UV/Hydrogen Peroxide, UV/Free Chlorine and UV/Chloramines Advanced Oxidation Process Treatment for Potable Reuse. *Water Res.* 2019, *164*, 114939.

(8) Zhang, Z.; Chuang, Y.-H.; Huang, N.; Mitch, W. A. Predicting the Contribution of Chloramines to Contaminant Decay during Ultraviolet/Hydrogen Peroxide Advanced Oxidation Process Treatment for Potable Reuse. *Environ. Sci. Technol.* 2019, *53*, 4416−4425.

(9) Chuang, Y.-H.; Chen, S.; Chinn, C. J.; Mitch, W. A. Comparing the UV/Monochloramine and UV/Free Chlorine Advanced Oxidation Processes (AOPs) to the UV/Hydrogen Peroxide AOP under Scenarios Relevant to Potable Reuse. *Environ. Sci. Technol.* 2017, *51*, 13859−13868.

(10) Chaplin, B. P. Critical Review of Electrochemical Advanced Oxidation Processes for Water Treatment Applications. *Environ. Sci. Process. Impacts* 2014, *16*, 1182−1203.

(11) Radjenovic, J.; Sedlak, D. L. Challenges and Opportunities for Electrochemical Processes as Next-Generation Technologies for the Treatment of Contaminated Water. *Environ. Sci. Technol.* 2015, *49*, 11292−11302.

(12) Jasmann, J. R.; Borch, T.; Sale, T. C.; Blotevogel, J. Advanced Electrochemical Oxidation of 1,4-Dioxane via Dark Catalysis by Novel Titanium Dioxide (TiO_2) Pellets. *Environ. Sci. Technol.* 2016, *50*, 8817−8826.

(13) Sirés, I.; Brillas, E.; Oturan, M. A.; Rodrigo, M. A.; Panizza, M. Electrochemical Advanced Oxidation Processes: Today and Tomorrow. A Review. *Environ. Sci. Pollut. Res.* 2014, *21*, 8336−8367.

(14) Gao, G.; Zhang, Q.; Hao, Z.; Vecitis, C. D. Carbon Nanotube Membrane Stack for Flow-through Sequential Regenerative Electro-Fenton. *Environ. Sci. Technol.* 2015, *49*, 2375−2383.

(15) Patra, S.; Munichandraiah, N. Electrochemical reduction of hydrogen peroxide on stainless steel. *J. Chem. Sci.* 2009, *121*, 675−683.

(16) Feng, Y.; Smith, D. W.; Bolton, J. R. Photolysis of Aqueous Free Chlorine Species (HOCl and OCl^-) with 254 nm Ultraviolet Light. *J. Environ. Eng. Sci.* 2007, *6*, 277−284.

(17) Zeng, T.; Plewa, M. J.; Mitch, W. A. *N*-Nitrosamines and Halogenated Disinfection Byproducts in U.S. Full Advanced Treatment Trains for Potable Reuse. *Water Res.* 2016, *101*, 176−186.

(18) Szczuka, A.; Berglund-Brown, J. P.; Chen, H. K.; Quay, A. N.; Mitch, W. A. Evaluation of a Pilot Anaerobic Secondary Effluent for Potable Reuse: Impact of Different Disinfection Schemes on Organic Fouling of RO Membranes and DBP Formation. *Environ. Sci. Technol.* 2019, *53*, 3166−3176.

(19) American Public Health Association, *Standard Methods for The Examination of Water and Wastewater*; 20th ed.; American Water Works Association & Water Environment Federation Washington: D.C., USA 1998.

(20) Bader, H.; Sturzenegger, V.; Hoigné, J. Photometric Method for the Determination of Low Concentrations of Hydrogen Peroxide by the Peroxidase Catalyzed Oxidation of N,N-Diethyl-p-Phenylenediamine (DPD). *Water Res.* 1988, *22*, 1109−1115.

(21) NDRL/NIST Solution Kinetics Database. http://kinetics.nist.gov/solution/ (retrieved March 20, 2020).

(22) Eberhardt, M. K.; Colina, R. The Reaction of OH Radicals with Dimethyl Sulfoxide. A Comparative Study of Fenton's Reagent and the Radiolysis of Aqueous Dimethyl Sulfoxide Solutions. *J. Org. Chem.* 1988, *53*, 1071−1074.

(23) Tai, C.; Peng, J.-F.; Liu, J.-F.; Jiang, G.-B.; Zou, H. Determination of Hydroxyl Radicals in Advanced Oxidation Processes

with Dimethyl Sulfoxide Trapping and Liquid Chromatography. *Anal. Chim. Acta* 2004, *527*, 73−80.
(24) Sahni, M.; Locke, B. R. Quantification of Hydroxyl Radicals Produced in Aqueous Phase Pulsed Electrical Discharge Reactors. *Ind. Eng. Chem. Res.* 2006, *45*, 5819−5825.
(25) Design Guidelines for the Selection and Use of Stainless Steel. https://www.nickelinstitute.org/media/1667/designguidelinesfortheselectionanduseofstainlesssteels_9014_.pdf (accessed Mar 22, 2020).
(26) Hokanson, D.; Trussell, S.; Dadakis, J.; Plumlee, M. H.; Fendorf, S.; Mitch, W. A. Evaluating Post Treatment Challenges for Potable Reuse Applications. *Water Research Foundation* 2020 Project Reuse-16-01/4780. ISBN: 978-1-60573-422-4.
(27) Fakhreddine, S.; Dittmar, J.; Phipps, D.; Dadakis, J.; Fendorf, S. Geochemical triggers of arsenic mobilization during managed aquifer recharge. *Environ. Sci. Technol.* 2015, *49*, 7802−7809.
(28) United States Environmental Protection Agency (USEPA). National Secondary Drinking Water Regulations (NSDWRs) https://www.epa.gov/sdwa/drinking-water-regulations-and-contaminants#Secondary (accessed Mar 20, 2020).
(29) Patton, S.; Li, W.; Couch, K. D.; Mezyk, S. P.; Ishida, K. P.; Liu, H. Impact of the Ultraviolet Photolysis of Monochloramine on 1,4-Dioxane Removal: New Insights into Potable Water Reuse. *Environ. Sci. Technol. Lett.* 2017, *4*, 26−30.
(30) Hamann, C. H.; Hamnett, A.; Vielstich, W. *Electrochemistry*; Second Ed.; Wiley-VCH: Weinheim, Germany.
(31) Chuang, Y. H.; Szczuka, A.; Mitch, W. A. Comparison of Toxicity-Weighted Disinfection Byproduct Concentrations in Potable Reuse Waters and Conventional Drinking Waters as a New Approach to Assessing the Quality of Advanced Treatment Train Waters. *Environ. Sci. Technol.* 2019, *53*, 3729−3738.

https://dx.doi.org/10.1021/acs.est.0c02144
Environ. Sci. Technol. 2020, 54, 12593−12601